Preparation and Electrocatalytic Properties of Nickel-Cobalt Metal Derivatives

Ying ZHANG [1], Yue HU [2] *, Bo YU [3]

[1] *School of Mechanical Engineering, Changchun Guanghua University, Changchun 130033, Jilin, China*
[2] *College of Physics and Electronic Engineering, Hebei Minzu Normal University, Chengde 067000, Hebei, China*
[3] *School of Mechanical and Electrical Engineer, Changchun Institute of Technology, Changchun 130012, Jilin, China*

http://doi.org/10.5755/j02.ms.39603

Received 28 November 2024; accepted 12 February 2025

At present, platinum is the most efficient electrocatalytic hydrogen evolution catalyst, which can effectively accelerate the kinetic reaction process of hydrogen evolution. Therefore, it is very important to develop a non-noble metal catalyst with low cost, high catalytic activity and high stability for hydrogen production from water electrolysis. Up to now, transition metal sulfides, oxides, carbides, nitrides and phosphates have been proven to have good electrocatalytic activity. Among them, bimetallic phosphates have become the research hotspot in this field because of their high catalytic activity compared with others. In this study, transition metal salts, urea and ammonium fluoride were used as raw materials for in situ growth of transition metal dihydrohydride $NiCo_2$/LDH on NF substrate based on hydrothermal reaction, the bimetallic phosphates $NiCo_2$/NF grown on the NF substrate were obtained. The experimental results show that the prepared $NiCo_2P$/NF catalyst exhibits excellent electrocatalytic performance. In alkaline media, a catal current density of 10 mA/cm^2 can be obtained at an overpotential of 97 mV, with a Tafel slope of only 21 mV/dec. Moreover, its electrocatalytic activity can be maintained for more than 10 h, which is consistent with the before the experiment. This is mainly attributed to: the $NiCo_2P$/NF derivative possesses the characteristics of a multimetal phosphide derived from transition metal elements Ni and Co after hydrothermal and phosphidation treatment. Its nanowire urchin-like heterostructure exposes more catalytically active sites, effectively promoting mass transfer and charge transfer accelerating the hydrogen evolution kinetics reaction process, and enhancing the catalytic performance with high catalytic stability.
Keywords: clean energy, water electrolysis for hydrogen production, catalytic electrode, transition metal phosphides, electrocatalytic activity.

1. INTRODUCTION

Since the 21st century, the two major issues of energy and environment have become burning hot, and the exploration and development of renewable clean has become a research hotspot [1]. Among various renewable energies, hydrogen is widely recognized as a green, efficient, and stable clean energy, and is an ideal substitute for traditional fuels. At present, although the global annual hydrogen production is large [2], most of it still uses traditional fuels to produce hydrogen, and the energy and problems have not been effectively solved. Therefore, the development of clean energy efficient hydrogen production technology has potential application value. Noble metal catalysts, despite their high HER catalytic activity, are limited in their application development due to their high cost and extremely low reserves.

Non-noble and non-metallic catalysts have been widely studied to explore alternatives to noble metal catalysts. So far, the transition metal compounds, including transition metal carbides [3], sulfides [4], phosphates [5], borides [6], selenides [7] and heteroatom-doped carbon materials formed by the combination of transition metal elements, are widely tested. Among various transition metal compounds, transition metal phosphides are the closest to Pt, making them a potential effective substitute for precious metals.

Up to now, transition metal phosphates are mostly in the form of powders, which have many disadvantages in conductivity, electrode preparation time and electrocatalytic stability [8]. The in-situ production of catalysts on metal substrates is considered as an effective solution, which can improve the conductivity of the catalyst while eliminating defects of the catalyst powder properties.

This study uses transition metal salts, urea, and ammonium fluoride as raw materials to generate transition metal hydroxide $NiCo_2$/LDH in-situ on NF substrates via hydrothermal reactions. After phosphating treatment, the bimetallic phosphide $NiCo_2P$/NF grown on the NF substrate is obtained.

Polarization curve tests were conducted using linear sweep voltammetry (LSV). Double-layer capacitance (C_{dl}) tests were performed using voltammetry (CV). Charge transfer kinetics during the HER process were investigated using electrochemical impedance spectroscopy (EIS), and the stability of the catalysts was studied using cyclic voltammetry and chronoamperometry.

The test results show that the prepared $NiCo_2P$/NF nanowire urchin-like heterostructure promotes mass transfer and charge transfer, accelerates the hydrogen evolution kinetics reaction process, and improves the catalytic performance. In a 1mol/L KOH electrolyte, an overpotential of only 97 mV is needed to achieve a catalytic current density of 10 mA/cm^2, with a Tafel slope of 121 mV/dec, and the electrocatalytic activity can be maintained for more than 10 h.

* Corresponding author: Y. Hu
E-mail: *jdhy@hbun.edu.cn*

2. EXPERIMENT

2.1. Raw material

The $NiCl_2·6H_2O$, $CoCl_2·6H_2O$, NaH_2PO_2, CH_4N_2, and KOH required for the experiment were all from Shanghai Aladdin Biochemical Technology Co., Ltd. The C_2H_6O was from National Medicine Chemical Re Co., Ltd. NH_4F was from XiLong Chemical Co., Ltd. The NF was from Changsha Linyuan New Material Co., Ltd. The H_2O was from Pall PURELAB TM Plus laboratory ultra-pure water from the USA. The Pt/C was from Shanghai Macklin Biochemical Technology Co., Ltd. The key elements and their proportions needed for the experiment are shown in Table 1.

Table 1. Key elements and ratio description of the experiment

Num	Key elements	Proportion
1	$CoCl_2·6H_2O$	2 mmol
2	$NiCl_2·6H_2O$	1 mmol
3	CH_4N_2O	10 mmol
4	NH_4F	1 mmol
5	Distilled water	50 ml
6	NaH_2PO_2	1 g

During the experimental process of designing and preparing nickel-cobalt metal derivatives, the following points should be noted: 1) select appropriate raw material and ensure the stability of material quality; 2) adhere to laboratory safety regulations and operating procedures, and wear personal protective equipment such as goggles, gloves, and laboratory; 3) ensure that the laboratory has adequate ventilation facilities to prevent the accumulation of toxic or harmful gases generated during the experiment from exceeding limits; 4) in the experimental operation steps, strictly control experimental parameters, record experimental data, and pay attention to any problems or unexpected situations that may arise during the process; 5) after the experiment is completed, the product needs to be thoroughly cleaned and dried to avoid moisture absorption or contamination during storage.

2.2. Synthesis of $NiCo_2$/LOH

The NF was immersed in 2 mol/l HCl solution and C_2H_6O solution, respectively, for about 30 min to remove the surface grease and oxide layer, after which the washed NF was cropped to 5 cm × 0.5 cm for use. Dissolve 2 mmol $CoCl_2·6H_2O$, 1 mmol $NiCl_2·6H_2O$, 10 mmol CH_4N_2O and 1 mmol NH_4F in 50 ml distilled water and stir evenly for about 30 min. The resulting liquid was slowly poured into the Teflon-lined autoclave containing NF, and then hydrothermally reacted at a high of 120 ℃ for 6 h, and then stopped and cooled to room temperature, to obtain the transition metal hydroxide $NiCo_2$/LDH grown in-situ on the foam nickel substrate.

2.3. Synthesis of $NiCo_2P$/NF

With NaH_2PO_2 as the phosphorus source, $NiCo_2$/LDH was placed upstream of the combustion boat, and 1 g NaH_2PO_2 was placed downstream of the combustion boat, with the upstream and downstream distinguished by the gas flow direction. Under the protection of the Ar atmosphere, the tubular furnace was heated to 300 ℃ at a heating rate of 15 ℃/min maintained for 2 h before natural cooling, and the bimetallic phosphide $NiCo_2P$/NF could be obtained.

2.4. Material characterization and electrocatalytic performance testing

X-ray diffraction (XRD) was used for phase analysis of $NiCo_2P$/NF, scanning electron microscopy (SEM) and transmission microscopy (TEM, HRTEM) were used for morphology and microstructure analysis of $NiCo_2P$/NF, and energy dispersive spectroscopy (EDS) was used for elemental composition analysis of $NiCo_2P$/NF.

Based on the three-electrode system, the catalytic performance of $NiCo_2P$/NF was tested using an electrochemical workstation (CHI), including polarization curve analysis using LSV, electrochemical active area analysis using double-layer capacitance (C_{dl}), charge transfer kinetics analysis using electrochemical impedance (EIS), and catalytic stability analysis using cyclic voltammetry and chronoamperometry.

3. RESULTS AND ANALYSIS

3.1. Phase analysis

The XRD patterns of the transition metal dihydrides $NiCo_2$/LDH and the transition metal phosphides $NiCo_2P$/NF are shown in Fig. 1.

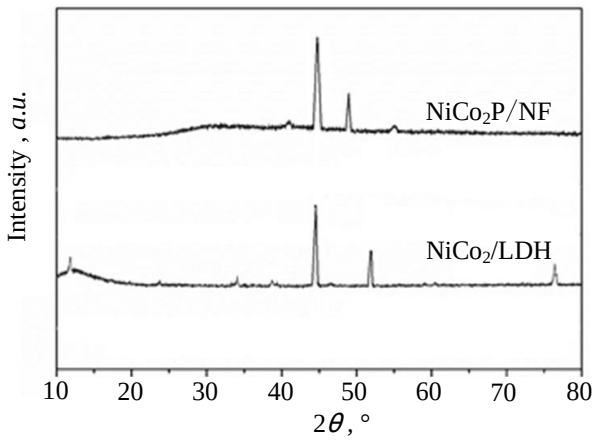

Fig. 1. The XRD patterns

Fig. 1 demonstrates that there are strong diffraction peaks at the positions of 2θ at 11.7°, 34.5°, 38.6°, 44.8°, 52.5° and 76.7°. The diffraction peaks correspond to (003), (009), (015), (021), (028) and (038) crystal faces of $NiCo_2$/LDH respectively (JCPDS card number: 03-0953) [9]. Fig. 1 demonstrates that the transition metal phosphates $NiCo_2P$/NF exhibit strong diffraction peaks at 2θ at 41.8°, 45.3°, 48.95° and 54.28°, the diffraction peaks correspond to (111), (201), (210) and (002) crystal faces of $NiCo_2P$/NF (JCPDS card number: 71-2336) [10] respectively, which indicates that $NiCo_2P$/NF materials have been successfully prepared.

The successful preparation of $NiCo_2$/LDH and $NiCo_2P$/NF in the above experimental results is completely in line with the experimental expectations which confirms that based on transition metal elements, multi-transition metal phosphides can be effectively prepared according to hydrothermal reaction, phosphating treatment and other treatment methods.

3.2. Morphology analysis

The morphology characterization of the transition metal dihydride $NiCo_2$/LDH and transition metal phosphide $NiCo_2P$/NF by XRD is shown in Fig. 2 and Fig. 3. The SEM image is magnified about 8000 times.

As shown in Fig. 2, the synthesized transition metal dihydrohydride $NiCo_2$/LDH exhibits a nanowire sea urchin-like structure with nanowires growing uniformly and densely on nickel foam with an elongated diameter of approximately 7 μm. The nanoseaurchin with a high-density nanowire composition has a larger surface area, which can expose more active sites, the three-dimensional porous skeleton provided by the foam nickel substrate makes the electron transfer rate at the active sites faster.

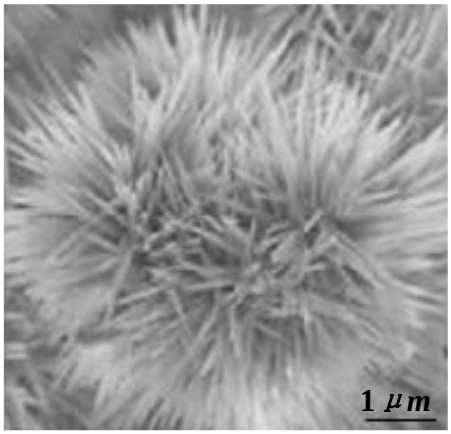

Fig. 2. SEM image of $NiCo_2$/LDH

As shown in Fig. 3, the transition metal phosphide $NiCo_2P$/NF generated by phosphating still maintains the nanowire sea urchin morphology of $NiCo_2$/LDH, without significant structural changes, which is attributed to the high stability of $Co(OH)_2$, allowing them to maintain its original structure after phosphating. After phosphating treatment, the diameter of $NiCo_2P$/NF grows to about 8 μm, which is larger than that of $NiCo_2$/LDH, indicating that after low-temperature phosphating, the diameter of the nickel-cobalt composite phosphide now increases, and the internal overlapping leaves more pores, which greatly increases the contact area between the electrode and the electrolyte, improving the diffusion of the electrolyte and migration of charges.

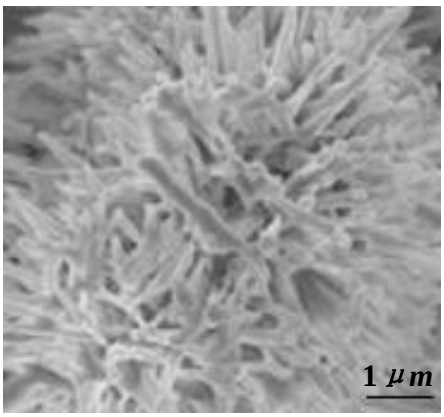

Fig. 3. SEM image of $NiCo_2P$/NF

The HRTEM image of $NiCo_2P$/NF is shown in Fig. 4, with clear lattice fringes and a spacing of 0.3 nm, corresponding to the (111) crystal plane of $NiCo_2P$ [11].

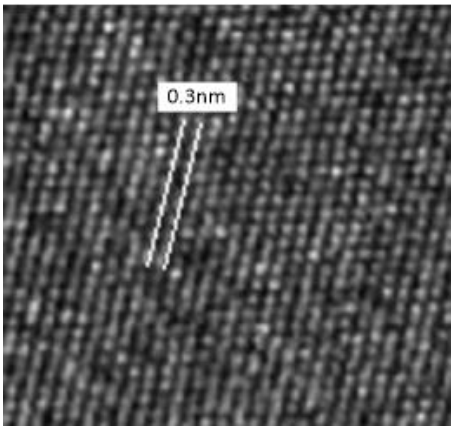

Fig. 4. HRTEM image of $NiCo_2P$/NF

Fig. 5 shows the HAD-STEM image of $NiCo_2P$, from which we can see that the sample is composed of multi-layered nanosheets, forming nanorods. These nanosheets significantly increase the specific surface area, enhancing the number of active sites. The active material grown on the surface increases the contact area with the electrolyte accelerating the charge transfer rate, and further improving the electrochemical performance.

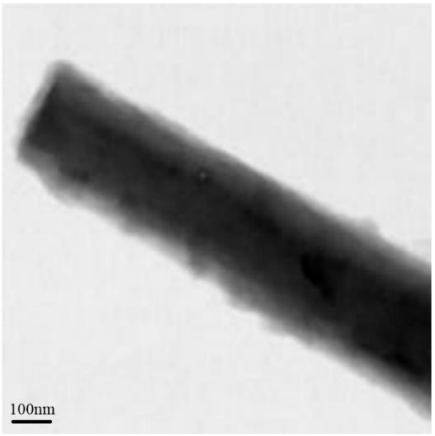

Fig. 5. HADDF-STEM image of $NiCo_2P$/NF.

The phase structure characteristics analysis of the experimental results of $NiCo_2$/LDH and $NiCo_2P$/NF are somewhat different from the expectations, mainly reflected in: 1) previously, the derivatives of $NiCo_2(CO_3)_{1.5}OH_3$ and NiCoP/NF prepared on hydrothermal reaction and phosphorization treatment have a nanorod array structure, but their exposed specific surface area is lower than that of $NiCo_2$/LDH and $NiCo_2P$/NF; 2) the prepared $NiCo_2P$/NF has a high degree of structural similarity with the precursor $NiCo_2$/LDH, and $NiCo_2P$/NF further elongates based on the nanourchin wire structure, which increases the reaction active sites and can effectively enhance the transfer rate and improve the electrochemical performance.

3.3. XPS analysis

The XPS patterns of $NiCo_2P$/NF are shown in Fig. 6, indicating that the elements of the sample include Ni, Co P, O, and C. It is speculated that the C element mainly

originates from incompletely converted hydroxide precursors.

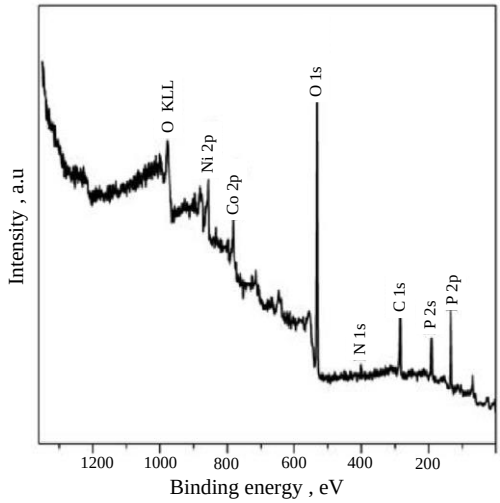

Fig. 6. XPS spectrum of $NiCo_2P$/NF

The high-resolution XPS spectrum of Ni 2p is shown in Fig. 7. It can be seen that two strong peaks at 863.1 eV and 882.3 eV appear in the Ni 2p region, corresponding to Ni $2p_{3/2}$ Ni $2p_{1/2}$, and satellite peaks appear at 867.2 eV and 881.7 eV [12].

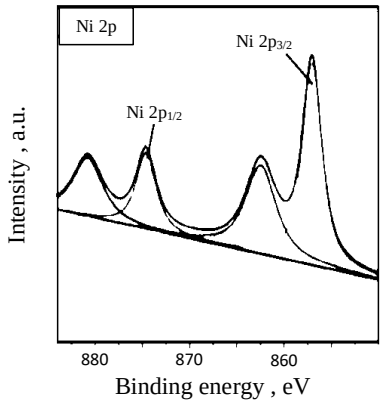

Fig. 7. HR-XPS spectra of Ni 2p

The high-resolution XPS spectrum of Co 2p is shown in Fig. 8, with two strong peaks appearing in the Co 2p region at 781.1 eV and 797.2 eV, corresponding to Co $2p_{3/2}$ and Co $2p_{1/2}$, respectively, and shifting towards higher energy, with satellite peaks appearing at 786.2 eV and 807.3 eV [13].

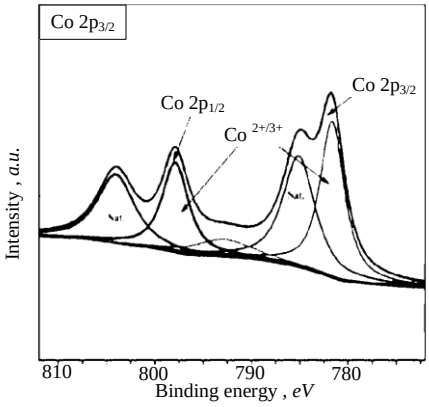

Fig. 8. HR-XPS spectra of Co 2p

The high-resolution XPS spectrum of P 2p is shown in Fig. 9, where 129.2 eV, 34.5 eV, and 133.5 eV correspond to P $2p_{3/2}$, P-O bonds, and P-C bonds, respectively, indicating significant electron transfer between $NiCo_2$ and NF, which is directly related to the promotion of electron transfer by the nanowire sea urchin spatial heterostructure.

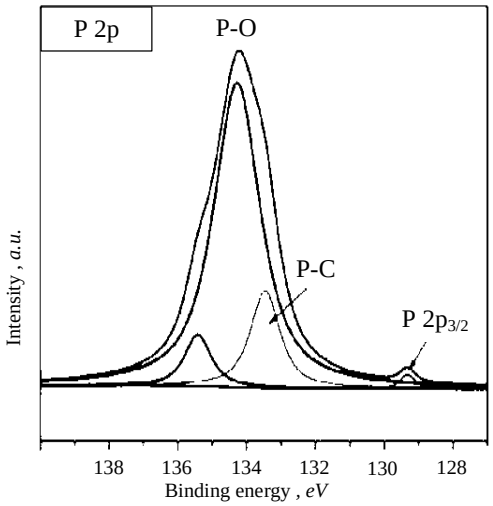

Fig. 9. HR-XPS spectra of P 2p

The XPS analysis results of the above experimental results for $NiCo_2$/LDH and $NiCo_2P$/NF are exactly as expected, are highly similar to the XPS analysis results of the $NiCo_2(CO_3)_{1.5}OH_3$ and NiCoP/NF derivatives prepared by thermal reaction and phosphorisation treatment, further confirming that the preparation of multi-transitional metal phosphides based on transitional metal elements, according to hydrothermal reaction and phosphization treatment, has obvious electronic interaction between the internal components, which effectively promotes electron transfer and improves the catalytic performance of the material.

3.4. Electrocatalytic evaluation

The electrocatalytic HER performance was evaluated by linear sweep voltammetry in an alkaline solution (1.0 mol/L KOH and PH = 14).

3.4.1. Linear scanning curve analysis

To allow for clear comparative analysis, linear sweep voltammetry tests were conducted at a current density of 10 mA/cm². The linear sweep voltammogram (LSV) in Fig. 10 shows that Pt/C requires only 1 mV overpotential at a density of 10 mA/cm², while $NiCo_2P$/NF needs 97 mV, indicating that under these conditions, the catalytic activity $NiCo_2P$/NF is far inferior to that of Pt/C.

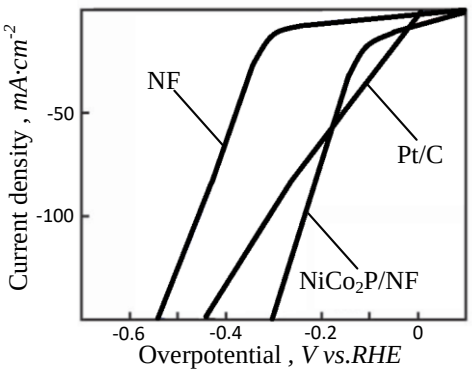

Fig. 10. LSV curves of Pt/C, $NiCo_2P$/NF and NF

However, as the potential continues to increase, the current density curve of $NiCo_2$/NF shows a rapid upward trend, which can be inferred that the catalytic performance of $NiCo_2P$/NF is expected to equal or even surpass Pt/C under specific conditions.

The overpotentials of other catalysts at a current density of 10 mA/cm^2 are shown in Table 2. These data demonstrate that the synthesized bimetallic phosphide $NiCo_2P$/NF exhibits outstanding catalytic performance.

Table 2. Analysis of catalyst

No	Name	Current density	Over-potential	References
1	$NiCo_2P$/NF	10 mA, cm^2	97 mV	This study
2	Co-VOx-P		98 mV	[14]
3	NiCoP/NF		105 mV	[15]
4	CoP3/CoMoP		110 mV	[16]
5	Co4Ni-P/NTs		129 mV	[17]
6	CoP/NiCop NTs		133 mV	[18]
7	NiCoP-300		150 mV	[19]
8	NiCoP/rGO		209 mV	[20]

3.4.2. Tafel slope analysis

The Tafel slope curves of Pt/C, $NiCo_2P$/NF, and NF are shown in Fig. 11, the values obtained from the analysis (in units of m/dec) are: 202, 121, and 56, respectively, that: the presence of the urchin-like spatially heterogeneous structure significantly enhances the electrocatalytic activity of $NiCo_2P$/NF compared to NF there is still a difference compared to Pt/C under the current conditions; the Tafel slope value of 21 mV/dec for $NiCo_2$/NF is sufficient to meet and follow the mer-Heyrovsky mechanismfor electrocatalytic hydrogen evolution reaction [21].

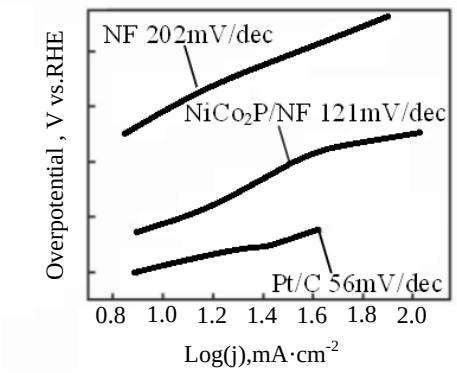

Fig. 11. Tafel slopes of catalysts

3.4.3. Analysis of active area and catalytic mechanism

Fig. 12 shows the CV curves obtained at different scan rates (80 m/s ~ 160 m/s) within the non-Fadaic potential window (-0.6 ~ -0.8 vs. RHE).

The difference in current density vs. scan rate curves and the C_{dl} values of $NiCo_2P$/NF and NF at a potential of -0.75 V were measured and are shown in Fig. 13. These results indicate that the ECSA and catalytic active sites of $NiCo_2P$/NF are far superior to those of NF, which is consistent with the previous analysis and further confirms the excellent performance of the $NiCo_2P$/NF nanowireurchin – like spatially heterogeneous structure.

3.4.4. Electrochemical impedance analysis

Fig. 14 shows the Nyquist plots of the electrochemical impedance of $NiCo_2P$/NF and NF. Compared with NF, thequist plot of $NiCo_2P$/NF is more compact, indicating that Rct($NiCo_2P$/NF) < Rct(NF), andCo_2P/NF has lower charge transfer impedance, thus having stronger charge transfer ability, which can effectively enhance the charge transfer rate and improve the kinetics of theytic reaction. This is completely consistent with the XPS analysis results.

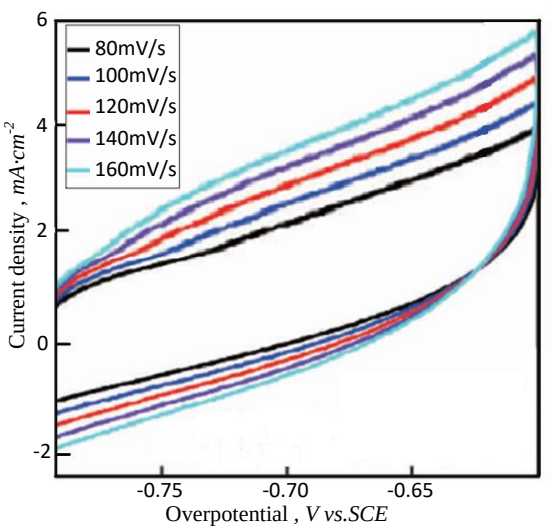

Fig. 12. CV curves of $NiCo_2P$/NF at different scan rates

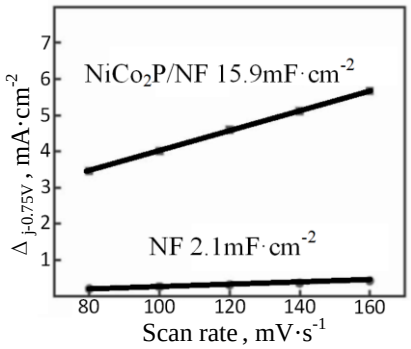

Fig. 13. The difference in the current density

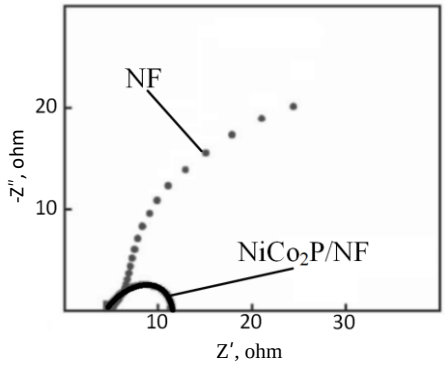

Fig. 14. Electrochemical impedance spectra (EIS) spectra

3.4.5. Electrochemical stability analysis

The electrocatalytic stability test curve is shown in Fig. 15 with a current density of 10 mA/cm² and a test time of 10 h. From the curve in Fig. 15, it can be seen that $NiCo_2P$/NF has stable catalytic activity in constant potential test.

Meanwhile, the catalyst $NiCo_2P$/NF was subjected to a

cyclic voltammetry stability test for 3000 cycles, the test data is shown in Fig. 16.

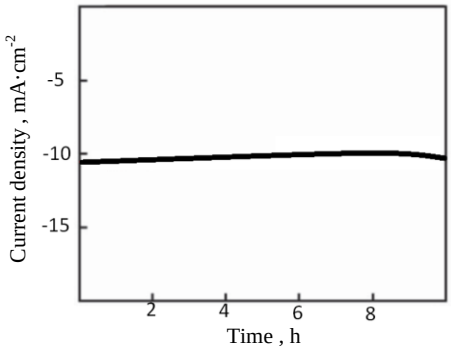

Fig. 15. Electrocatalytic stability test curve

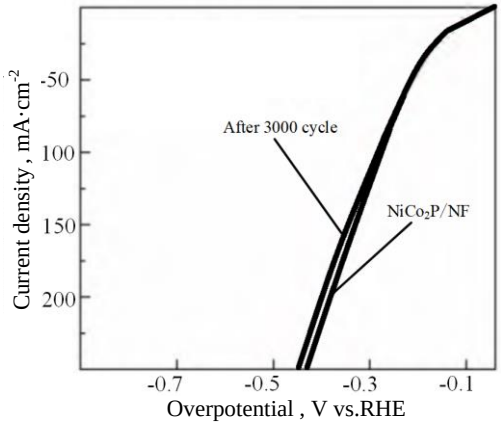

Fig. 16. Polarization curves before and after CV test

From the analysis of the curve in Fig. 16, it can be seen that the LSV curves $NiCo_2P$/NF before and after the test are almost coincident, which further indicates that the catalyst $NiCo_2P$/NF has high catalytic and satisfactory long-term durability.

According to the above electrochemical test results, $NiCo_2P$/NF has excellent catalytic performance, which may be due to the morphology of the prepared samples leading to higher activity, allowing for lower overpotentials to provide higher current densities, lower internal resistance leading to faster charge transfer rates, ECSA (exposing more active catalytic sites), and the 3D large/medium pore sea urchin-like structure promoting the transport of active substances the release of bubbles.

The above experimental results show that the electrochemical performance analysis of $NiCo_2P$/NF is approximately the same as the experimental expectations. Previously prepared NiCoP/NF derivatives based on hydrothermal reactions and phosphating treatments have been proven to have good electrocatalytic performance and electrochemical stability. In this study, the $NiCo_2P$/NF transition metal phosphide was prepared and evaluated by linear voltammetry, Tafel plots, Nyquist, and electrocatalytic activity tests, confirming that $NiCo_2P$/NF also has excellent electrocatalytic performance. Therefore, the above common conclusions confirm that based on transition metal elements, the preparation of multimetallic phosphides by hydrothermal reactions and phosphating treatments has excellent electrocatalytic performance.

4. CONCLUSIONS

1. Based on hydrothermal reaction, transition metal hydroxide $NiCo_2$/LDH was grown in situ on the nickel foam substrate and after phosphating treatment, bimetallic phosphide $NiCo_2P$/NF grown on the nickel foam substrate was obtained. The electrocatalytic test shows that at a current density of 10 mA/cm^2, its overpotential is 97 mV, the Tafel slope is only 11 mV/dec, and the activity can be maintained for more than 10 h, which confirms that the bimetallic phosphide NiCoP/NF has good electrocatalytic performance, and it meets the expectations before the experiment.
2. Characterization techniques analysis: 1) the prepared $NiCo_2P$/NF derivatives possess the characteristics of multi-metal phosph derived from transition metal elements Ni and Co after hydrothermal reaction and phosphorization treatment, with a heterostructure of nanowire sea urchin, significantly increasing the number of exposed catalytic active sites; 2) XPS analysis reveals that the heterostructure of nanowire sea urchin can mass transfer and charge transfer between $NiCo_2P$ and NF; 3) the linear voltammogram, Tafel plot, and Nyquist plot demonstrate that heterostructure of $NiCo_2P$/NF effectively promotes water dissociation, accelerates the electrocatalytic hydrogen evolution kinetics, thereby enhancing its electrocytic performance in various aspects.
3. This study successfully prepared the $NiCo_2P$/NF catalyst with a nanowire urchin-like heterostructure, and completed the effective evaluation of the $NiCo_2P$/NF catalyst using modern evaluation techniques. The research results further confirm that the multimetal phosphides derived from transition elements Ni and Co after hydrothermal reaction and phosphating treatment have good electrocatalytic performance. Meanwhile, this study has certain theoretical value for the research of catalytic materials for clean energy preparation and also enriches the application of transition metal phosphides in clean energy preparation.

Acknowledgments

This work is funded by Science Research Project og Hebei Education Department (No. ZC2025127).

REFERENCES

1. **Yu, B., Li, Y., Fu, X.N., Yu, L., Fu, H.D., Cao, Y.X., Chen, Z.H.** Preparation and electrocatalytic Oxygen Evolution of Bimetallic Phosphates $(NiFe)_2P$/NF *Green Processing and Synthesis* 13 (1) 2024: pp. 1 – 10. https://doi.org/10.1515/GPS-2023-0266
2. **Balat, M.** Potential Importance of Hydrogen as a Future Solution to Environmental and Transportation Problems *International Journal of Hydrogen Energy* 33 (15) 2008: pp. 4013 – 4029. https://doi.org/10.1016/j.ijhydene.2008.05.047
3. **Xing, J.N., Li, Y., Guo, S.W., Jin, T., Li, H.X., Wang, Y.H., Jiao, L.F.** Molybdenum Carbide In-Situ Embedded into Carbon Nanosheets as Efficient Bifunctional Electrocatalysts for Overall Water Splitting *Electrochim Acta* 298 2019: pp. 305 – 312. https://doi.org/10.1016/j.electacta.2018.12.091

4. **Zhang, J., Wang, T., Liu, P., Liu, S.H., Dong, R.H., Zhuang, X.D., Chen, M.W., Feng, X.L.** Engineering Water Dissociation Sites in MoS_2 Nanosheets for Accelerated Electrocatalytic Hydrogen Production *Energy & Environmental Science* 9 (9) 2016: pp. 2789 – 2793. https://doi.org/10.1039/C6EE01786J
5. **Wu, Y.Q., Liu, S.M., Jin, S.J., Yan, Y.Q., Wang, Z., Chen, L.H. Su, B.L.** Synthesis of Zn-Doped NiCoP Catalyst with Porous Double-layer NanoarrayStructure and Its Electrocatalytic Properties for Hydrogen Evolution *Chemical Journal of Chinese Universities* 42 (8) 2021: pp. 2483 – 2492. https://doi.org/10.7503/cjcu20210218
6. **Chen, X.C., Yu, Z.X., Wei, L., Zhou, Z., Zhai, S.L., Chen, J.S., Wang, Y.Q., Huang, Q.W., Karahan, H., Liao, X.Z., Chen, Y.** Ultrathin Nickel Boride Nanosheets Anchored on Functionalized Carbon Nanotubes as Bifunctional Electrocatalysts for Overall Water Splitting *Journal of Materials Chemistry A* 7 (2) 2019: pp. 764 – 774. https://doi.org/10.1039/C8TA09130G
7. **Kong, D.S., Wang, H.T., Lu, Z., Yi, C.** $CoSe_2$ Nanoparticles Grown on Carbon Fiber Paper: An Efficient and Stable Electrocatalyst for Hydrogen Evolution Reaction *Journal of the American Chemical Society* 136 (13) 2014: pp. 4897 – 4900. https://doi.org/10.1021/ja501497n
8. **Tian, Y.M., Sheng, D., Shi, Z.Q.** Self-supported Electrocatalysts for Advanced Energy Conversion Processes *Materials Today* 19 (5) 2016: pp. 265 – 273. https://doi.org/10.1016/j.mattod.2015.10.012.
9. **Chen, H., Hu, L.F., Chen, M., Yan, Y., Wu, L.** Nickel-Cobalt Layered Double Hydroxide Nanosheets for High-performance Supercapacitor Electrode Materials *Advanced Functional Materials* 24 (7) 2014: pp. 934 – 942. https://doi.org/10.1002/adfm.201301747
10. **Tong, M., Wang, L., Yu, P., Liu, X., Fu, H.G.** 3D Network Nanostructured NiCoP Nanosheets Supported on N-Doped Carbon Coated Ni Foam as a Highly Active Bifunctional Electrocatalyst for Hydrogen and Oxygen Evolution Reactions *Frontiers of Chemical Science and Engineering* 12 (3) 2018: pp. 417 – 424. https://doi.org/10.1007/s11705-018-1711-1
11. **Ding, L., Shu, Y., Wang, A., Zheng, L.L., Wang, X.D., Zhang, T.** Preparation and catalytic Performances of Ternary Phosphides NiCoP for Hydrazine Decomposition *Applied Catalysis a-General* 385 (1 – 2) 2010: pp. 232 – 237. https://doi.org/10.1016/j.apcata.2010.07.020
12. **Lin, Y., Sun, K., Chen, X., Chen, C., Pan, Y., Li, X.Y., Zhang, J.** High-precision Regulation Synthesis of Fe-doped Co_2P Nanorod Bundles as Efficient Electrocatalysts for Hydrogen Evolution in All-pH Range and Seawater *Journal of Energy Chemistry* 55 2021: pp. 92 – 101. https://doi.org/10.1016/j.jechem.2020.06.073
13. **Zhou, P., Zhuai, G., Lv, X., Liu, Y.Y., Wang, Z.Y., Wang, P., Zheng, Z.K., Cheng, H.F., Dai, Y., Huang, B.B.** Boosting the Electrocatalytic HER Performance of Ni_3N-V_2O_3 via the Interface Coupling Effect *Applied Catalysis B: Environmental* 283 2021: pp. 119590. https://doi.org/10.1016/j.apcatb.2020.119590
14. **Zhu, Z., Xu, K., Guo, W., Zhang, H.Y., Xiao, X., He, M.S., Yu, T.T., Zhao, H., Zhang, D.E., Yang, T.** Vanadium-phosphorus Incorporation Induced Interfacial Modification on Cobalt Catalyst and its Super Electrocatalysis for Water Splitting in Alkaline Media *Applied Catalysis B: Environmental* 304 2022: pp. 120985. https://doi.org/10.1016/J.APCATB.2021.120985
15. **Duan, J., Chen, S., Vasil, E.A., Qiao, S.Z.** Anion and Canon Modulation in Metal Compounds for Bifunctional Overall Water Splitting *ACS Nano* 10 (9) 2016: pp. 8738 – 8745. https://doi.org/10.1021/acsnano.6b04252
16. **Jiang, D., Xu, Y., Yang, R., Li, D., Meng, S., Chen, M.** CoP_3/CoMoP Heterogeneous Nanosheet Arrays as Robust Electrocatalyst for pH-Universal Hydrogen Evolution Reaction *ACS Sustainable Chemistry & Engineering* 7 (10) 2019: pp. 9309 – 9317. https://doi.org/10.1021/acssuschemeng.9b00357
17. **Sivanantham, A., Ganesan, P., Shanmugam, S.** Hierarchical $NiCo_2S_4$ Nanowire Arrays Supported on Ni Foam: An Efficient and Durable Bifunctional Electrocatalyst for Oxygen and Hydrogen Evolution Reactions *Advanced Functional Materials* 26 (26) 2016: pp. 4661 – 4672. https://doi.org/10.1002/adfm.201600566
18. **Tahir, M., Pan, L., Idrees, F., Zhang, X.W., Wang, L., Zou, J.J., Wang, Z.L.** Electrocatalytic Oxygen Evolution Reaction for Energy Conversion and Storage: A Comprehensive Review *Nano Energy* 37 2017: pp. 136 – 157. https://doi.org/10.1016/j.nanoen.2017.05.022
19. **Xiao, C., Li, Y., Lu, X., Zhao, C.** Bifunctional Porous NiFe/$NiCo_2O_3$/Ni Foam Electrodes with Triple Hierarchy and Double Synergies for Efficient Whole Cell Water Splitting *Advanced Functional Materials* 26 (20) 2016: pp. 3515 – 3523. https://doi.org/10.1002/adfm.201505302
20. **Wang, J., Xu, F., Jin, H.Y., Chen, Y., Wang, Y.** Non-Noble Metal-based Carbon Composites in Hydrogen Evolution Reaction: Fundamentals to Applications *Advanced Materials* 29 (14) 2017: pp. 1605838. https://doi.org/10.1002/adma.201605838
21. **Zhang, L., Zhang, J., Fang, J., Wang, X., Yin, L., Zhu, W., Zhuang, Z.** Cr-Doped CoP Nanorod Arrays as High-Performance Hydrogen Evolution Reaction Catalysts at High Current Density *Small* 17 (28) 2021: pp. 2100832. https://doi.org/10.1002/smll.202100832